*Supporting Information for:*

# Surface-Clean, Phase-Pure Multi-Metallic Carbides for Efficient Electrocatalytic Hydrogen Evolution

Shuang Gao[a,b], Hui Chen[a], Yipu Liu[a], Guo-Dong Li[a], Ruiqin Gao[a] Xiaoxin Zou[a]*

a *State Key Laboratory of Inorganic Synthesis and Preparative Chemistry, College of Chemistry, Jilin University, Changchun 130012, P. R. China*

b *Key Laboratory of Preparation and Application of Environmental Friendly Materials (Jilin Normal University), Ministry of Education, Changchun, 130103, China*

\* Corresponding author. E-mail address: xxzou@jlu.edu.cn (X. Zou)

## Theoretical calculation

All calculations were performed using the *Vienna Ab-initio Simulation Package* (VASP)[1,2], and the generalized gradient approximation (GGA) with the Perdew–Burke–Ernzerhof (PBE) [3]exchange–correlation functional was used with the projector augmented wave method[4]. For all theoretical models, the cutoff energy was 400 eV, the convergence threshold was set as $10^{-4}$ eV in energy and 0.05 eV $Å^{-1}$ in force. The Brillouin zones were sampled by Monkhorst–Pack[5] $3 \times 3 \times 3$ and $3 \times 3 \times 1$ k-point grid for geometric optimization of bulk and slab models, and $5 \times 5 \times 1$ k-point grid was used to calculate the DOS of slab models. The symmetrization was switched off and the dipolar correction was included. The correction of van der Waals interaction was included using the DFT-D2 method[6]. All structures were fully relaxed to the ground state and spin-polarization was not considered in all calculations. We chose (001) surface to investigate the d-band center of $Co_6Mo_6C$ and $\beta$-$Mo_2C$. For $Co_3Mo_3C$, there were six different termination of (001) facet. We built $1 \times 1$ repeat cell with 15 Å vacuum layer, and the upper a quarter of atom layers were fully relaxed and the remaining were kept frozen during computational process. We calculated their surface energy and chose the best stable surface to compare d-band center with the (001) facet of $\beta$-$Mo_2C$ with Mo-termination. The surface energy was calculated by:

$$\gamma = \frac{E^{relaxed}_{slab} - nE_{bulk}}{A} - \frac{E^{unrelaxed}_{slab} - nE_{bulk}}{2A}$$

where $E^{relaxed}_{slab}$ and $E^{unrelaxed}_{slab}$ is energy of relaxed and unrelaxed of slab model, respectively. $A$ is surface area of slab model and $E_{bulk}$ is energy of bulk model.
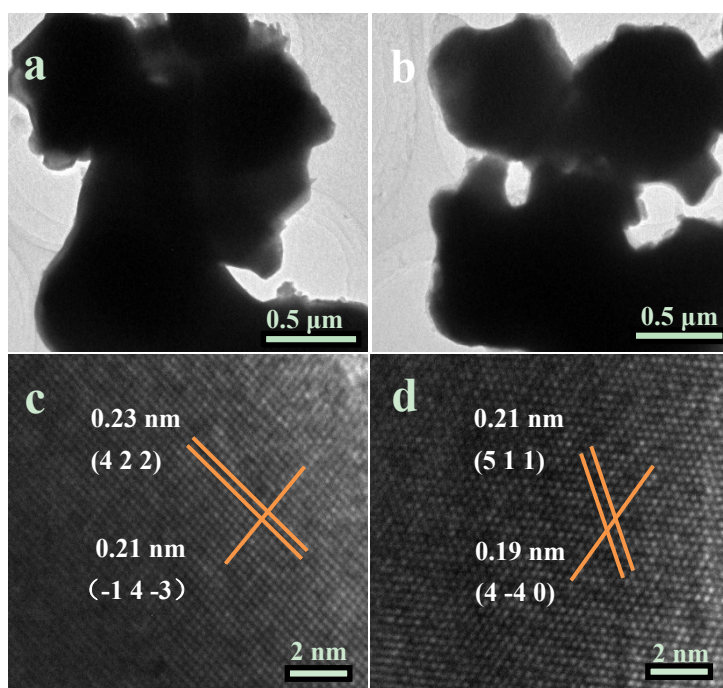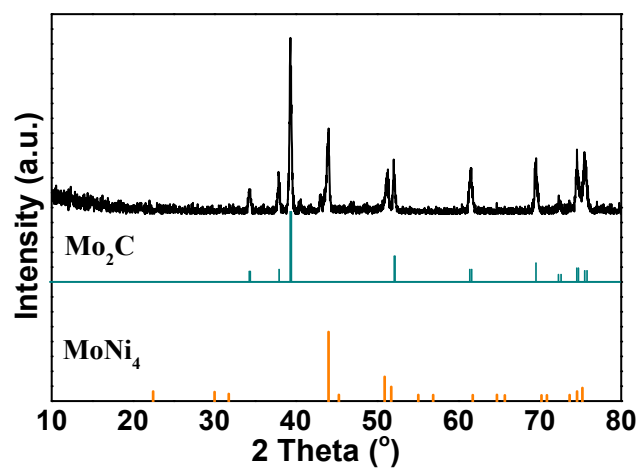
**Figure S1** XRD patterns of nickel molybdenum compounds.



**Figure S2** (a,b) TEM images and (c,d) HRTEM images of Co$_3$Mo$_3$C after HER cycles.
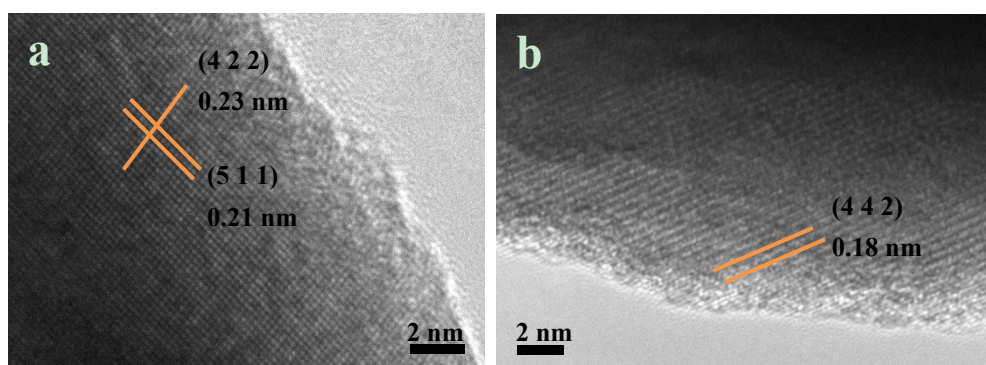
**Figure S3** (a) TEM image of $Co_3Mo_3C$, (b) TEM image of $Co_6W_6C$
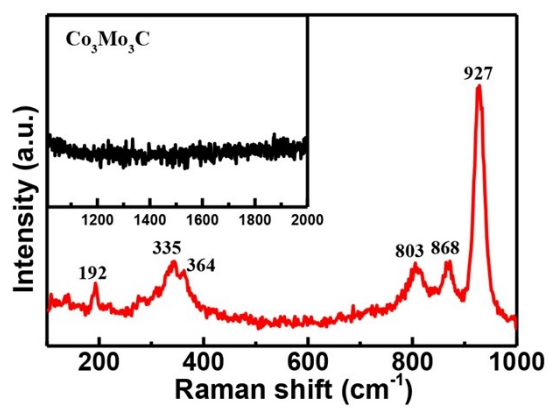


**Figure S4** Raman spectrum of $Co_3Mo_3C$
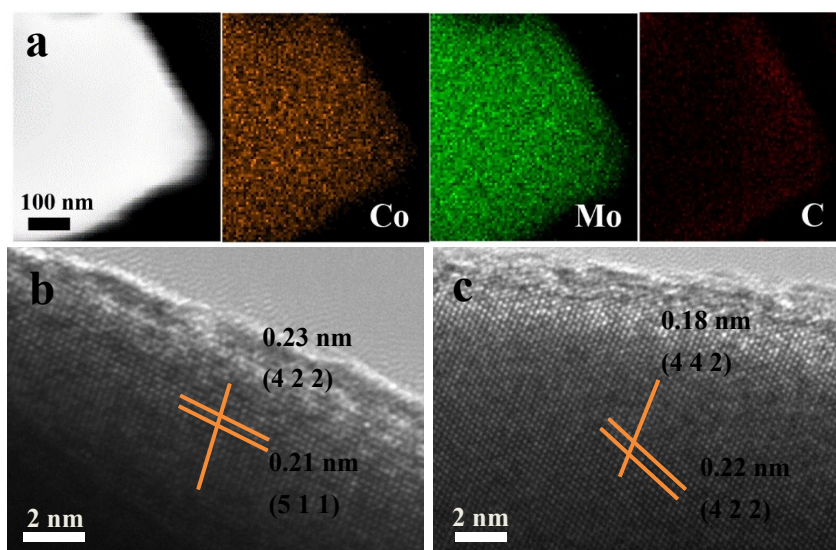
**Figure S5** (a) STEM image and corresponding elemental mapping images of $Co_3Mo_3C$. (b) HRTEM image of $Co_xFe_{3-x}Mo_3C$, (c) HRTEM image of $Co_xFe_{6-x}W_6C$.
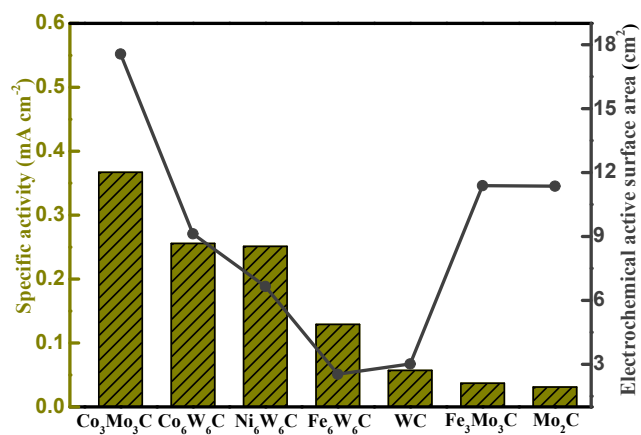
**Figure S6** Comparison of electrochemical active surface areas (ECSAs) and ECSA-normalized specific activities of these multi-metallic carbides (evaluated at an overpotential of 300 mV).
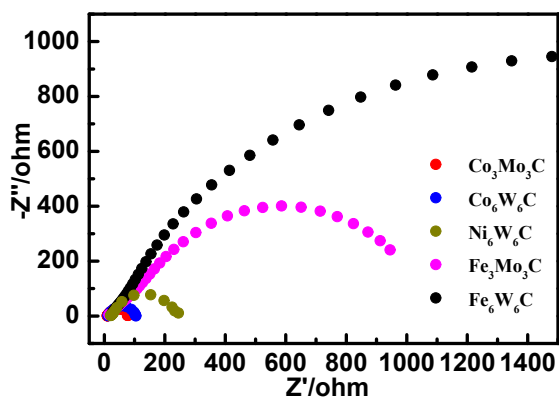
**Figure S7** Electrochemical impedance spectroscopy (EIS) Nyquist plots of these bimetallic carbides.



Mo
Co
C

a

b

3.653 J/m²
I

3.923 J/m²
II

3.897 J/m²
III

3.871 J/m²
IV

4.043 J/m²
V

3.848 J/m²
VI
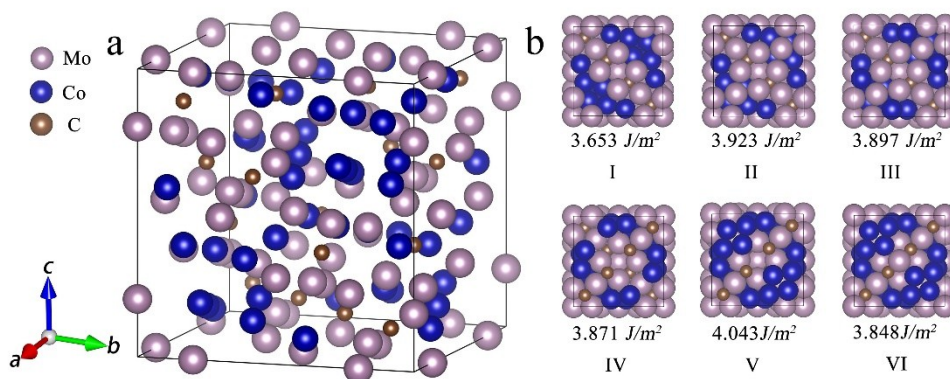
Figure S8 (a) the bulk structure of Co₃Mo₃C. (b) the different termination of (001) facet of Co₃Mo₃C and the corresponding surface energies

**Table S1** Electrical conductivity of different multi-metallic carbides.

| Sample | $Co_3Mo_3C$ | $Fe_3Mo_3C$ | $Co_6W_6C$ | $Ni_6W_6C$ | $Fe_6W_6C$ | $Co_xFe_{3-x}Mo_3C$ | $Co_xFe_{6-x}W_6C$ | $Mo_2C$ | WC |
|---|---|---|---|---|---|---|---|---|---|
| Conductivity ($S\ cm^{-1}$) | 159.2 | 15.4 | 48.3 | 7.5 | 6.2 | 12.8 | 5.9 | 12.4 | 5.6 |

**Table S2** Comparison of the electrocatalytic activity of $Co_3Mo_3C$ with some representative solid-state HER

| Catalyst | Electrolyte | Current density ($j$) | Overpotential at the corresponding $j$ | Reference |
|---|---|---|---|---|
| $Co_3Mo_3C$ | 1 M KOH | 1 mA/cm$^2$<br>10 mA/cm$^2$ | 72 mV<br>169 mV | this work |
| Ni-Mo | 2 M KOH | 10 mA/cm$^2$ | 80 mV | 7 |
| MoB | 1 M KOH | 10 mA/cm$^2$ | 225 mV | 8 |
| $Mo_2C$ | 1 M KOH | 10 mA/cm$^2$ | 185 mV | 8 |
| MoP | 0.5 M $H_2SO_4$ | 10 mA/cm$^2$ | 246 mV | 9 |
| $CoS_2$ | 0.5 M $H_2SO_4$ | 10 mA/cm$^2$ | 192 mV | 10 |
| MoNiNC | 0.1 M KOH | 10 mA/cm$^2$ | 110 mV | 11 |
| $Ni_3ZnC_{0.7}$ | 1 M KOH | 10 mA/cm$^2$ | 93 mV | 12 |
| $Co_6Mo_6C$-G | 0.5 M $H_2SO_4$ | 10 mA/cm$^2$ | 154 mV | 13 |
| $Co_6Mo_6C$ NSs/G | 0.5 M $H_2SO_4$ | 10 mA/cm$^2$ | 73 mV | 14 |

catalysts recently reported.

References for SI Section

1. Kresse, G.; Furthmüller, J.; Efficiency of ab-initio total energy calculations for metals and semiconductors using a plane-wave basis set. Comput. Mater. Sci., 1996, 6, 15-50.

2. Kresse, G.; Furthmüller, J.; Efficient iterative schemes for ab initio total-energy calculations using a plane-wave basis set. Phys. Rev. B, 1996, 54, 11169-11186.

3. Perdew, J. P.; Burke, K.; Ernzerhof, M.; Generalized Gradient Approximation Made Simple. Phys. Rev. Lett., 1996, 77, 3865-3868.

4. Blöchl, P. E.; Projector augmented-wave method. Phys. Rev. B, 1994, 50, 17953-17979.

5. Monkhorst, H. J.; Pack, J. D. Special points for Brillouin-zone integrations. Phys. Rev. B, 1976, 13, 5188-5192.

6. Grimme, S. J.; Semiempirical GGA‐type density functional constructed with a long‐range dispersion correction. Comp. Chem. 2006, 27, 1787-1799.

7. McKone, J. R.; Sadtler, B. F.; Werlang, C. A.; Lewis, N. S.; Gray, H. B.; Ni–Mo Nanopowders for Efficient Electrochemical Hydrogen Evolution. *ACS Catal.*, 2013, 3, 166-169.

8. Vrubel, H.; Hu, X.; Molybdenum Boride and Carbide Catalyze Hydrogen Evolution in both Acidic and Basic Solutions. Angew. Chem. Int. Ed., 2012, 51, 12875-12878.

9. Chen, X.; Wang, D.; Wang, Z.; Zhou, P.; Wu, Z.; Jiang, F.; Molybdenum phosphide: a new highly efficient catalyst for the electrochemical hydrogen evolution reaction. Chem. Commun., 2014, 50, 11683-11685.

10. Faber, M. S.; Lukowski, M. A.; Ding, Q.; Kaiser, N. S.; Jin, S.; Earth-Abundant Metal Pyrites (FeS$_2$, CoS$_2$, NiS$_2$, and Their Alloys) for Highly Efficient Hydrogen Evolution and Polysulfide Reduction Electrocatalysis. J. Phys. Chem. C, 2014, 118, 21347-21356.

11. Wang, F.; Sun, Y.; He, Y.; Liu, L.; Xu, J.; Zhao, X.; Yin, G.; Zhang, L.; Li, S.; Mao, Q.; Huang, Y.;

Zhang, T.; Liu, B.; Highly efficient and durable MoNiNC catalyst for hydrogen evolution reaction. Nano Energy, 2017, 37, 1-6.

12. Wang, Y.; Wu, W.; Rao, Y.; Li, Z.; Tsubaki, N.; Wu, M.; Cation modulating electrocatalyst derived from bimetallic metal–organic frameworks for overall water splitting. J. Mater. Chem. A, 2017, 5, 6170-6177.

13. He, C.; Tao, J.; Three-dimensional hollow porous $Co_6Mo_6C$ nanoframe as an highly active and durable electrocatalyst for water splitting. J. Catal., 2017, 347, 63-71.

14. He, C.; Tao, J.; 2D $Co_6Mo_6C$ Nanosheets as Robust Hydrogen Evolution Reaction Electrocatalyst. Adv. Sustainable Syst., 2017, 2, 1700136.